J. Phys. A: Math. Gen. **30** (1997) 5065–5075. Printed in the UK PII: S0305-4470(97)81449-7

Modular groups, visibility diagram and quantum Hall effect

Yvon Georgelin†, Thierry Masson‡ and Jean-Christophe Wallet†

† Division de Physique Théorique§, Institut de Physique Nucléaire, F-91406 ORSAY Cedex, France

‡ Laboratoire de Physique Théorique et Hautes Énergies‖, Université de Paris-Sud, Bât 211, F-91405, Orsay Cedex, France

Received 30 January 1997

Abstract. We consider the action of the modular group $\Gamma(2)$ on the set of positive rational fractions. From this, we derive a model for a classification of fractional (as well as integer) Hall states which can be visualized on two 'visibility' diagrams, the first one being associated with even denominator fractions whereas the second one is linked to odd denominator fractions. We use this model to predict, among some interesting physical quantities, the relative ratios of the width of the different transversal resistivity plateaus. A numerical simulation of the tranversal resistivity plot based on this last prediction fits well with the present experimental data.

1. Introduction

Since the discovery of the two-dimensional quantized Hall conductivity by [1] for the integer plateaus and by [2] for the fractional ones, the quantum Hall effect has been an intensive field of theoretical and experimental investigations.

The pioneering theoretical contributions [3a–c] relating the basic features of the hierarchy of the Hall plateaus with the properties of a two-dimensional incompressible fluid with fractional charges collective excitations [3a] have triggered further works dealing with condensed matter theory [4], quantum field theory¶ and mathematical physics [5]. It appears now that the two-dimensional electron system in the quantum Hall regime is associated with a complicated phase diagram with a lot of possible transitions between the various phases, whose better understanding deserves further experimental and theoretical studies.

As far as the theoretical viewpoint is concerned, two important elements underlying numerous works can be singled out: (i) the flux attachment transformation relating quantum Hall states [6] for which the Chern–Simons theory is a suitable field theory framework; (ii) the hierarchical structure of the set of Hall states [7]$^{+}$ where particle-hole symmetry plays an important role. The combination of the above elements into a Chern–Simons–Landau–Ginzburg theory has led the authors of [8] to propose a topology of the phase diagram (in

§ Unité de Recherche des universités Paris 11 et Paris 6 associée au CNRS.

‖ Laboratoire associé au CNRS, URA D0063.

¶ We have in mind models related to Chern–Simons theory, Coulomb gas approach and rational conformal field theories; see [4] and references therein.

$^{+}$ Given a basis of Laughlin states, one can obtain elements of the set of Hall states through condensation of quasiparticles of other elements of the set.

0305-4470/97/145065+11$19.50

the external magnetic field-disorder plane) together with an attempt to explain the possible origin of superuniversality ruling the considered transitions.

It appears that (at least some of) the above ideas can be formulated in term of modular transformations, that is, discrete symmetry transformations acting on some parameter space of the quantum Hall system and pertaining to the modular group or one of its subgroups. Modular transformations in the framework of quantum Hall effect have been considered from different viewpoints [9].

Recently [10], two of us constructed a classification of the quantum Hall states based on arithmetical properties of the group $\Gamma(2)$ of modular transformations acting on the three cusps $\{i\infty\}$, $\{0\}$ and $\{1\}$ of its fundamental domain in the Poincaré half plane. The proposed classification reproduces and refines the Jain hierarchical one [11]. In particular, it has obtained families of quantum Hall fluid states (plus the insulator state), each family being generated from a metallic state labelled by an even denominator fraction $\lambda = (2s+1)/2r$.

The purpose of this paper is to extract more algebraic properties linked with this classification, then to translate them into a graphical representation, called the visibility diagram [12] which generates Farey sequences [13] together with an associated diagram called the dual diagram. From this analysis, we predict a global organization of the various Hall conductivity states stemming from the action of $\Gamma(2)$ as well as some important quantitative features of the Hall fractional conductivity plateaus such as the relative ratios of their width (at least for a not too strong applied magnetic field). Furthermore, we obtain from a numerical construction a transverse resistivity plot which fits very well with the experimental data.

The paper is organized as follows. In section 2 we present useful material underlying our classification of the quantum Hall states. In section 3, we introduce the visibility diagram together with its associated dual diagram in connection with the quantum Hall effect. The corresponding physical information encoded in these diagrams is discussed in section 4 where we also confront a numerical simulation of the resistivity plot stemming from our construction to the experimental data. Finally, we summarize our results and conclude in section 5.

2. The group $\Gamma(2)$ and the quantum Hall states

In this section, we summarize the essential tools that will be needed in the sequel as well as some of the main results of the previous work [10] to which we refer for more details.

Let $\mathcal{P}$ be the upper complex plane and z be a complex coordinate on $\mathcal{P}$ ($\mathrm{Im}z > 0$). We recall that the inhomogeneous modular group $\Gamma(1)$ (=PSL$(2, Z)$) is the set of transformations G acting on $\mathcal{P}$ and defined by:

$$G(z) = \frac{az+b}{cz+d} \qquad a, b, c, d \in Z \qquad ad - bc = 1 \qquad \text{(unimodularity condition)}. \tag{2.1}$$

The modular group $\Gamma(1)$ has two generators given by:

$$T(z) = z + 1 \qquad S(z) = -\frac{1}{z}. \tag{2.2}$$

The group $\Gamma(2)$ that will be the building block of the following construction is a subgroup of $\Gamma(1)$. $\Gamma(2)$ is known in mathematical literature as the principal congruence unimodular group at level 2. It is the set of transformations G acting on $\mathcal{P}$ defined by

$$\text{equation (2.1)} \qquad a \text{ and } d \text{ odd} \qquad b \text{ and } c \text{ even}. \tag{2.3}$$

$\Gamma(2)$ is a free group generated by

$$T^2(z) = z + 2 \qquad \Sigma(z) = ST^{-2}S(z) = \frac{z}{2z+1}. \tag{2.4}$$

For more mathematical properties of $\Gamma(2)$, see, for example [14]. Here, we notice that $\Gamma(2)$ is a common subgroup of two other subgroups of $\Gamma(1)$ which have already been considered from different viewpoints in connection with the quantum Hall effect. The first one, $\Gamma_S(2)$, is generated by T^2 and S and is the natural symmetry group of the Landau problem on the torus; it appears in the construction of the many-body Landau states on the torus [16] in terms of the Coulomb gas vertex operators [16]. The second subgroup of $\Gamma(1)$, $\Gamma_T(2)$, which contains $\Gamma(2)$, is related to the similarity transformations used by Jain in his hierarchical model [11]. Recall that $\Gamma_T(2)$ is generated by T and Σ.

Transformations $G \in \Gamma(2)$ can be written as

$$G(z) = \frac{(2s+1)z + 2n}{2rz + (2k+1)} \tag{2.5}$$

where $k, n, r, s \in Z$ satisfy the unimodularity condition

$$(2s+1)(2k+1) - 4rn = 1. \tag{2.6}$$

Now, identify any fraction $z = p/q$ with a filling factor and select a given Hall metallic state labelled by $\lambda = \frac{(2s+1)}{2r}$ with $r \geqslant 0, s \geqslant 0$. As shown in [10], there is a family of transformations $G^{\lambda}_{n,k} \in \Gamma(2)$ (with n and k still satisfying (2.6)) which sends $z = \mathrm{i}\infty$ onto λ. Then, from the images $G^{\lambda}_{n,k}(0)$ and $G^{\lambda}_{n,k}(1)$ of 0 and 1 by the transformations $G^{\lambda}_{n,k}$, one obtains a (Jain-like) hierarchy of Hall states surrounding the metallic state λ on the resistivity plots.

For example, the double Jain family $J^{i}_{1/2}$ of states surrounding the metallic state $\lambda = \frac{1}{2}$

$$J^{+}_{1/2} = \tfrac{1}{3}, \tfrac{2}{5}, \tfrac{3}{7} \qquad \ldots N/(2N+1) \tag{2.7a}$$

$$J^{-}_{1/2} = \tfrac{2}{3}, \tfrac{3}{5}, \tfrac{4}{7} \qquad \ldots N/(2N-1) \tag{2.7b}$$

can be easily recovered in our scheme from the images $G^{1/2}_{n,k}(0)$ and $G^{1/2}_{n,k}(1)$ with respectively $n \geqslant 0$ for (2.7*a*) and $n < 0$ for (2.7*b*). Notice that the construction separates the even numerator Hall fractions from the odd numerator one so that it may be possible to take into account a possible particle-hole symmetry within the present scheme. Other families surrounding any metallic state (fraction with even denominator) can be constructed in the same way so that all the experimentally observed Hall states can be taken into account in the present construction. This will be discussed further in section 4.

In the next section, we will be concerned with a diagrammatic description of the classification of the quantum Hall states which permits one to visualize the global organization of the various Hall conductivity states stemming from the action of $\Gamma(2)$. To reach this goal, we first introduce a convenient parametrization of the transformations $G^{\lambda}_{n,k}$. Indeed, it can easily be verified that the $G^{\lambda}_{n,k}$'s, for fixed $\lambda = (2s+1)/2r$, can be recast into the form

$$G^{\lambda}_{m}(z) = \frac{(2s+1)z + 2m(2s+1) + 2b}{2rz + 2m(2r) + 2d + 1} \tag{2.8}$$

where m is any integer and b and d are also arbitrary integers satisfying the unimodularity condition

$$(2s+1)(2d+1) - 4rb = 1. \tag{2.9}$$

For a given λ, fixing b, d and varying m from $-\infty$ to ∞, a complete hierarchy of states is recovered as before [10] from $G^{\lambda}_{m}(0)$ and $G^{\lambda}_{m}(1)$. Furthermore, one has

$$\lim_{m\to\pm\infty} G^{\lambda}_{m}(z) = \lambda \tag{2.10}$$

which reflects the fact that the sequence of Hall fluid fractions converges to the fraction λ labelling a given metallic state which defines that sequence. This point has to be compared with the general topology of the recently proposed phase diagrams for the quantum Hall effect where, roughly, each metallic state (even denominator state) appears to be surrounded by a definite family of Hall liquid states (odd denominator states). We will discuss this point in section 4.

From the above parametrization (2.8), we now construct a shift operator $A^{\lambda} \in \Gamma(2)$ corresponding to each metallic state λ, which acts on the fluid states (and possibly on the insulator state $\nu = 0$). We define this shift operator A^{λ} (which depends only on λ) as the following operator product

$$A^{\lambda} = G^{\lambda}_{m+1} \circ (G^{\lambda}_{m})^{-1} \tag{2.11}$$

whose action is given by

$$A^{\lambda}(z) = \frac{(1-2(2r)(2s+1))z + 2(2s+1)^2}{-2(2r)^2 z + 1 + 2(2s+1)2r}. \tag{2.12}$$

The action of A^{λ} to a given rational fraction p/q equal to $G^{\lambda}_{m}(0)$ or $G^{\lambda}_{m}(1)$ gives another rational fraction equal respectively to $G^{\lambda}_{m+1}(0)$ or $G^{\lambda}_{m+1}(1)$, so that A^{λ} acts as a shift operator, raising the number m by one unit. The inverse operator $(A^{\lambda})^{-1}$ performs the corresponding lowering in m.

The operators A^{λ} satisfy the following relations

$$A^{\lambda}(z) = z \iff z = \lambda \tag{2.13}$$

$$\mathrm{Tr}[A^{\lambda}] = 2 \tag{2.14}$$

$$\det[A^{\lambda}] = 1 \tag{2.15}$$

where $[A^{\lambda}]$ denotes the two-by-two matrix corresponding to the modular transformation A^{λ}. Equations (2.14) and (2.15) are just a mere consequence of the definition of the group $\Gamma(2)$. Notice that (2.14) reflects the parabolic nature of the transformations A^{λ} which means that A^{λ} may have no more than two fixed points (which must be necessarily real [14]). Therefore, equation (2.13) means that the metallic state $\lambda = (2s+1)/2r$ is actually the unique fixed point for the shift operator A^{λ}. This last property may be extended to the case where $r = 0$, which corresponds to the point at infinity on the real axis.

3. Visibility diagram and dual diagram

We are now in position to introduce a diagrammatic description that we find particularly useful and predictive for the classification of the quantum Hall states. This diagrammatic tool, which permits one to obtain quantitative results on the different quantum Hall states is called the 'visibility diagram' and has already been used in other areas of physics [12]. We will also introduce another diagram, hereafter called the dual diagram, which will allow us to extract in a straightforward way some of the information encoded in the visibility diagram.

3.1. The visibility diagram

This diagram is a simple pictorial device for the construction of Farey sequences [13] of rational numbers, each one being associated to a given vertex of a two-dimensional square lattice.

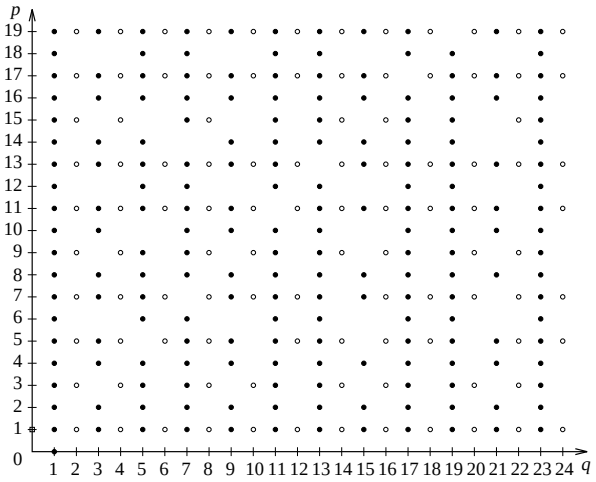

Figure 1. Visibility diagram. Full dots correspond to odd denominator fractions whereas open dots indicate even denominator fractions.

Let us consider the two-dimensional square lattice depicted in figure 1 where the vertices are indexed by a couple of positive or null relatively prime integers (q, p). Since the action of $\Gamma(2)$ preserves the even or odd nature of q and since a special role is played by the even denominator fractions in the sequel, we find it convenient to use different symbols (see figure 1) to separate the vertices belonging to a row with q even from those belonging to a q odd row. Therefore, the visibility diagram is made of the vertices of couples (q, p) of positive integers which are not hidden by any other vertex for an observer located at the origin $(0, 0)$. Notice that the origin is not considered as a visible point.

It is known in arithmetics that all the Farey-ordered sequences $F_n, (n = 1, 2, \ldots)$ of rational fractions p/q with p positive and $0 \leqslant q \leqslant n$ are in one-to-one correspondence with the visible vertices $(q, p), 0 \leqslant q \leqslant n$. Strictly speaking, for any Farey sequence F_n, p and q are required to satisfy $p \leqslant n$ and $q \neq 0$; here, since we are considering applying the above machinery to the fractional quantum Hall effect, we relax the above requirement somehow, thus allowing fractions with $p > n$ (and formally the 'infinite fraction' $\infty \equiv 1/0 \iff (0, 1)$).

Corresponding to this identification, the group $\Gamma(2)$ acts on the vertices of the visibility diagram in a rather simple way: it is actually represented by the linear action of two-by-two matrices on the two components (q, p) of the vertices, a property we will use in the following.

Now, it is easy to draw on the visibility diagram each family of vertices corresponding to the previously introduced fractions $G_m^\lambda(0)$ and $G_m^\lambda(1)$.

Let us describe in detail what kind of picture we obtain (see figure 2). First, for a given $\lambda = (2s + 1)/2$, $r = 1$, the quantum Hall rational numbers $G_m^\lambda(0)$ and $G_m^\lambda(1)$, where m is any integer, are all located on each parallel side of distinct unbounded bevelled left-end side stripes. The two sides of each stripe start from the vertices $(1, s)$ and $(1, s + 1)$ and

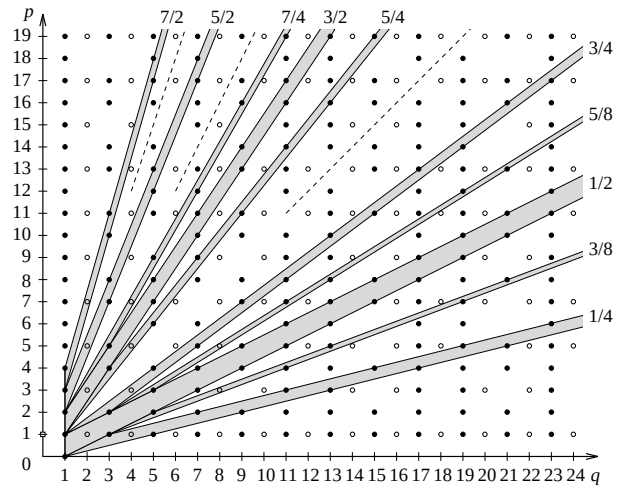

Figure 2. Even denominator stripes structure.

their slope is equal to $\lambda = (2s+1)/2$, as it can be easily seen by using for instance (2.8) and (2.9) from which one obtains after some algebra the equations defining the two parallel sides of the stripes. They are given in the (q, p) plane by $P = (\frac{2s+1}{2})Q \mp \frac{1}{2}$ where the minus (resp. plus) sign refers to the side starting from the vertex $(1, s)$ (resp. $(1, s+1)$). This agrees with the generation mechanism we gave previously for each Jain-type family [10]; recall that, as far as the action of $\Gamma(2)$ is concerned, the couple of cusps $(\{s\}, \{s+1\})$ may be substituted into the equivalent couple $(\{0\}, \{1\})$. The metallic state λ itself is shown to be surrounded on the visibility diagram by the family of fluid states (and eventually by the insulator whenever $\lambda = \frac{1}{2}$) it generates. We will call such families ($\lambda = (2s+1)/2$) the principal stripes ($r = 1$).

Glued on each side of any principal stripe there is an infinite number of other secondary, tertiary... stripes ($r = 2, 3 \ldots$). They are all similar in shape to a principal one: two infinite parallel sides, a bevelled left-end side and each one labelled by a metallic state $\lambda = (2s+1)/2r$. The states $G^{\lambda}_{m}(0)$ and $G^{\lambda}_{m}(1)$, with m being any integer, are all located on the parallel sides of the stripe λ in such a way that each metallic state finds itself isolated from the other metallic states by the members of its family on a stripe of slope λ. Starting from the secondary stripes ($r = 2$), it is possible to construct families of tertiary stripes, quartenary stripes etc, families of stripes of any order. The equations defining the two sides of a stripe of order r are easily derived from (2.8) and (2.9). They are given in the (q, p) plane by $P = (\frac{2s+1}{2r})Q \mp \frac{1}{2r}$. A pecularity appears in the diagram concerning the Hall insulator state ($\nu = 0$). Its vertex representation is $(1, 0)$; clearly it pertains to a given family λ, only for $\lambda = 1/2r (r \geqslant 1)$. This last property could have some importance for a possible direct phase transition between that state and another state. The reader has certainly noticed that the quadrant $p \geqslant 0, q \geqslant 0$ is not completely covered by stripes, a (half) stripe-shaped region is left uncovered, it is defined by $p \geqslant 0, 0 \leqslant q \leqslant 1$. We shall also come back to this last pecularity.

On any fraction of any given stripe λ acts as the step operator A^{λ} or its inverse in such a way that the metallic state $\lambda = (2s+1)/2r$ located at the lattice vertex $(2r, 2s+1)$ is a fixed point for A^{λ}. The fluid states (and eventually the insulator state) on the edge of the corresponding stripe are all transformed among themselves under that action, any of them

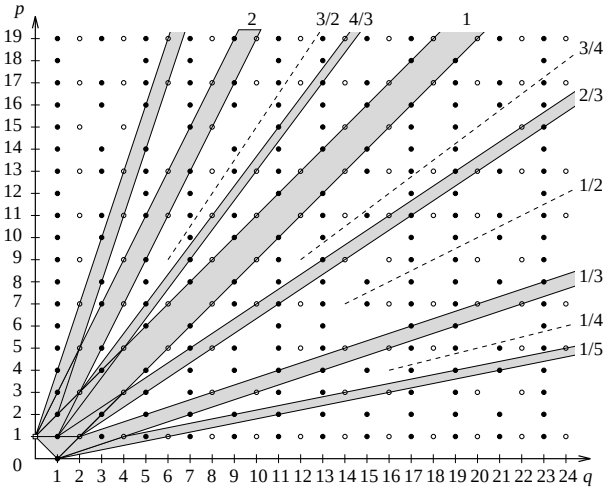

Figure 3. Odd denominator stripes structure.

is in fact the image of a $G_m^\lambda(0)$ or a $G_m^\lambda(1)$ under some power of A^λ and its inverse. In fact, all the information encoded in this diagram can be thoroughly reproduced by using the A^λ's and $(A^\lambda)^{-1}$'s. This can be rephased by saying that the A^λ's are the algebraic counterpart of the graphical representation of the (tree-like) structures formed by the Hall states on the above diagram.

3.2. The dual diagram

Observe that the previous structure on the visibility diagram is a mere consequence of a well known theorem in arithmetics which states that, for any given two relatively prime positive integers p and q, there exist two other (necessarily relatively prime) positive integers a and b satisfying $pb - qa = 1$ or $pb - qa = -1$. Using this theorem, it is now easy to realize that the set of (a, b) pairs stemming from these latter equations, for fixed (p, q) and q even, are all located on the two sides of the stripe labelled by $\lambda = \frac{p}{q}$ depicted in figure 2.

But one could instead consider q odd so that another structure can be obtained in the visibility diagram where now stripes labelled by $\lambda = \frac{p}{q}$ with q odd can be defined as shown in figure 3. We will call this resulting structure the dual diagram. Indeed, it can easily be seen that any stripe in figure 2 corresponds to a given direction on the dual diagram (depicted by dotted lines in figure 3), and conversely. This diagram will prove to be useful at evaluating the relative ratios of the width of the Hall plateaus.

4. Physical discussion

We are now in position to extract some physical information from the two diagrams that have been defined. We first identify any fraction p/q with the filling factor ν (what we implicitly assumed in the previous sections). This picture suggests that the $\Gamma(2)$ symmetry transformations act on some parameter space describing the quantum Hall system. Recall that the metallic (resp. liquid) states are labelled by fractions with an even (resp. odd) denominator.

First, keeping in mind the above identification, it is obvious that our construction treats

integer and fractional states on an equal footing. Now, consider the structure given in figure 2. One observes that each principal stripe bears a self-similar branched structure built from that stripe and all its descendants. Notice that the resulting global organization of the states in the stripes agrees quite well with the experimentally observed one. We point out that our construction predicts the existence of an infinite number of families with a self-similar (tree-like) structure. As far as the present experimental situation is concerned, (see [17]), the Jain family $\lambda = \frac{1}{2}$ corresponding in figure 2 to the stripe with the largest width, has the most numerous well established observed states ($N_{obs} \approx 13$). The other observed families labelled respectively by $\lambda = \frac{3}{2}, \frac{1}{4}, \frac{3}{4}, \frac{5}{2}, \frac{5}{4}$ and corresponding respectively to stripes of decreasing width are associated to a decreasing number of observed states (respectively $N_{obs} \approx 7, 6, 5, 4$). Roughly speaking, this suggests that the width of a stripe may be related to the (experimental) difficulty to observe the associated states. Notice that the insulator state $\nu = 0$ ($= 0/1$ in our picture) does not label any stripe on any of both diagrams.

Now consider the action of the two generators of $\Gamma(2)$ given in (2.4) on the visibility diagram. T^2 can be interpreted as a Landau shift operator and Σ corresponds to a flux attachment operator. On the visibility diagram, the action of T^2 on a vertex (q, p) gives rise to a vertical shift $(q, p) \to (q, p + 2q)$ whereas the action of Σ on (q, p) produces a horizontal shift $(q, p) \to (q + 2p, p)$. Since flux attachment can be obtained by magnetic field variation, a variation of the magnetic field is associated on the visibility diagram with a corresponding horizontal shift. Observe now that the stripes of the dual diagram are labelled by fractions with odd denominators, each of which correspond to a plateau in the Hall conductivity. Bringing this all together, this suggests identifying (up to an overall dimensionful factor) the 'horizontal' width of any stripe of the dual diagram, defined by the intercept of any horizontal line, with that stripe with the width of the corresponding plateau. Notice that both integer and fractional plateaus are involved in this picture as already mentioned at the beginning of this section.

It is a straightforward computation to show that the 'horizontal' width of any stripe labelled by $\lambda = p/q$ is equal to $2/p$. Then, the above identification leads to a prediction of all the ratios of the widths of the Hall plateaus given by

$$\frac{\gamma(\nu_1 = p_1/q_1)}{\gamma(\nu_2 = p_2/q_2)} = \frac{p_2}{p_1} \tag{4.1}$$

where $\gamma(\nu)$ denotes the width of the plateau labelled by ν and can be expressed as

$$\gamma(\nu = p/q) = \frac{2}{p}\gamma_0 \tag{4.2}$$

where the overall parameter γ_0 has the dimension of a magnetic field. At this point, one important remark is in order. It is well known that the width of the plateaus decreases when the temperature increases so that for sufficiently high temperatures the classical behaviour for the Hall resistivity is recovered. Therefore, if the above identification is correct, equation (4.1) should be valid only at zero temperature.

Nevertheless, one might already expect to obtain a reasonably good agreement with the present (non-zero temperature) experimental data. In order to check this, we have confronted prediction (4.1) with an experimental resistivity plot [18]. To do this, we have to fix two parameters. The first one is the width of a *given* transverse resistivity plateau which will determine the value of γ_0. In the present numerical analysis, we choose to fit this value with the $\nu = \frac{3}{2}$ experimental plateau. The second parameter is the position of the centre of *this chosen* plateau on the 'to be determined' resistivity plot. We assume that this plateau is centred around its corresponding filling factor value $\nu = \frac{3}{2}$. These two requirements will determine completely all the widths and positions on the other plateaus. The numerical result

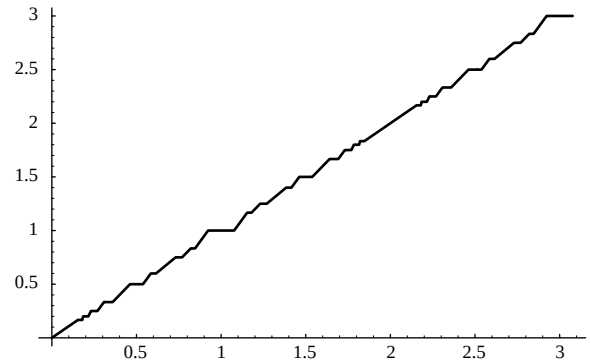

Figure 4. Numerical determination of the transverse resistivity plot. The horizontal (resp. vertical) axis corresponds to filling factor ν (resp. tranverse resistivity in unit h/e^2).

is shown in figure 4 and exhibits a good agreement with the corresponding experimental plot (figure 5).

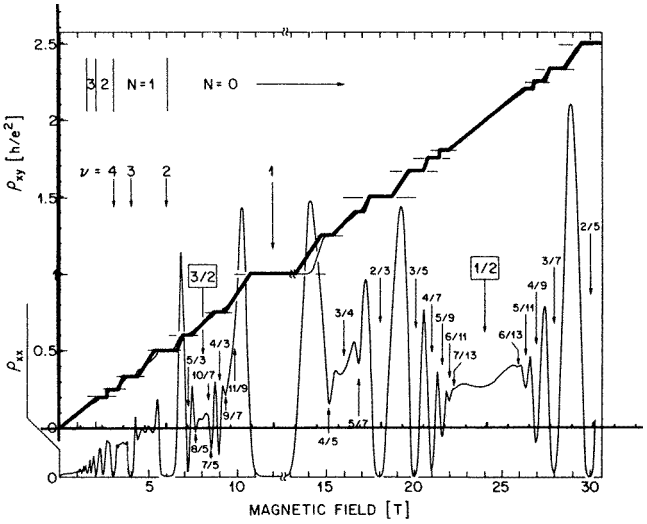

Figure 5. Our resistivity plot simulation (heavy curve) compared with the classical measurements of [17] (light curves).

5. Conclusion

In this paper we have exploited some arithmetic properties linked with the classification of the quantum Hall states stemming from the action of $\Gamma(2)$. These properties can be well synthetized in a graphical representation based on a visibility diagram, in which the resulting global organization of all the quantum Hall states is found to form (tree-like) self-similar structures. In particular, this structure is in complete agreement with the (experimental) hierarchy of observed states.

Furthermore, we used some of the arithmetic properties rooted in this construction

together with a physical interpretation of the two generators of $\Gamma(2)$ to conjecture the (zero temperature) ratios of the widths of the Hall plateaus. Moreover, this suggests in particular that the zero temperature values of these ratios are universal. We tried to confront the predictions obtained from this conjecture to the present (non-zero temperature) experimental data by constructing numerically the corresponding resistivity plot. This latter is in good agreement with some experimental resistivity plot (see figure 5).

As has already been mentioned in this paper, the $\Gamma(2)$ transformations could be understood as an infinite set of discrete transformations acting on some parameter space of the quantum Hall system. Therefore, it should be interesting to use this $\Gamma(2)$ symmetry to construct a model for the quantum Hall effect, for instance in the spirit of [8] and first of [9]. On the other hand, it should also be interesting to incorporate the $\Gamma(2)$ symmetry into a renormalization group framework to study the possible relations it induces among the fixed points that might provide some new insight into the possible origin of the superuniversality property shared by the observed transitions between Hall states. These questions are presently being studied.

Acknowledgments

We are indebted to A Comtet, M Dubois-Violette, J Mourad and S Ouvry for valuable discussions.

References

[1] von Klitzing K, Dorda G and Pepper M 1980 *Phys. Rev. Lett.* **45** 494
[2] Tsui D C, Störmer H L and Gossard A C 1982 *Phys. Rev. Lett.* **48** 1559
[3a] Laughlin R B 1983 *Phys. Rev. Lett.* **50** 1395
[3b] Haldane F D M 1983 *Phys. Rev. Lett.* **51** 605
[3c] Halperin B I 1984 *Phys. Rev. Lett.* **52** 1583
[4] For a review, see, e.g. Stone M 1992 *Quantum Hall Effect* (Singapore: World Scientific)
[5] Connes A 1990 *Géométrie Non Commutative* (Paris: InterEditions)
For a review, see, e.g. Bellissard J, van Elst A and Schulz-Baldes H 1994 *J. Math. Phys.* **35** 5373
[6] Girvin S M and MacDonald A H 1987 *Phys. Rev. Lett.* **1252** 58
Read N 1989 *Phys. Rev. Lett.* **62** 86
Lopez A and Fradkin E 1991 *Phys. Rev.* B **44** 5246
Zhang S C, Hanson T H and Kivelson S 1989 *Phys. Rev. Lett.* **82** 62
[7] See [3b] and [3c]
Jain J K 1989 *Phys. Rev. Lett.* **63** 199
[8] Kivelson S, Dung-Hai Lee and Zhang S C 1992 *Phys. Rev.* B **46** 2223
[9] See, e.g. Fradkin E and Kivelson S 1996 *Nucl. Phys.* B **474** 543
Burgess C P and Lütken C A 1996 *MacGill Preprint* McGill-96/39
Burgess C P and Lütken C A 1996 *Prepint* cond-mat/9611118
Pryadko L P and Zhang S C 1995 *Preprint* cond-mat/9511140
[10] Georgelin Y and Wallet J C 1997 *Phys. Lett.* A **224** 303
[11] Jain J K 1990 *Phys. Rev.* B **41** 7653
See also third of [8]
[12] Allen T 1983 *Physica* **6D** 305
Fröhlich J and Thiran E 1996 Visibility diagram have also been used previously in the fractional Hall effect from a somehow different viewpoint *Preprint* (Zürich: ETH) ETH-TH/96-22 unpublished
[13] For Farey sequences theory see Hardy G H and Wright E M 1968 *An Introduction to the Theory of Numbers* (Oxford: Clarendon)
[14] Mumford D 1983 *Tata Lectures on Theta (vols I, II, III)* (Boston, MA: Birkhauser)

See also Schoeneberg B 1974 *Elliptic Modular Functions, An Introduction* (Berlin: Springer)

[15] Haldane F D M and Rezayi E H 1985 *Phys. Rev.* B **31** 2529

[16] Christofano G, Maiella G, Musto R and Nicomedi F 1991 *Phys. Lett.* B **262** 88

[17] Willet R L, Eisenstein J P, Störmer H L, Tsui D C, Gossard A C and English J H 1988 *Phys. Rev. Lett.* **61** 997 and references therein

See also Jain J K 1995 *Talk presented at the XXXV Cracow School of Theoretical Physics (Zakopane, Poland, June)*

Jain J K 1995 *Acta Phys. Pol.* **26** 2149 and references therein

[18] Willett R *et al* 1987 *Phys. Rev. Lett.* **59** 1776